Monte Carlo and lattice-dynamics studies of the thermal and elastic properties of a rigid-ion model of sodium chloride

Zhaoxin Gong and G. K. Horton
Serin Physics Laboratory, Rutgers–The State University of New Jersey, P.O. Box 849, Piscataway, New Jersey 08855-0849

E. R. Cowley
Department of Physics, Camden College of Arts and Sciences, Rutgers–The State University of New Jersey, Camden, New Jersey 08102
(Received 13 June 1988)

We have calculated the thermodynamic properties and elastic constants of a rigid-ion model of sodium chloride, at zero pressure, using a combination of Monte Carlo simulations at high temperatures (300–1050 K) and anharmonic perturbation theory at low temperatures. While the results were intended as a benchmark for the simple model we have used, the agreement with experiment is remarkably good.

I. INTRODUCTION

In this paper we report benchmark results on the thermal and elastic properties of a rigid-ion model of a typical solid alkali halide, NaCl, using a combination of anharmonic perturbation theory and Monte Carlo simulation. A combination of this type has been shown to be capable of providing a complete description of the corresponding properties of the inert-gas solids, for either a simple Lennard-Jones model,[1,2] or for more realistic potentials.[3–5] The alkali halides are probably the next-simplest materials to study, and good experimental data are available for them. We have shown previously that anharmonic perturbation theory can give an excellent description at low to moderately high temperatures.[6,7]

In the interests of simplicity, we have used a rigid-ion model of sodium chloride, in which contributions to the interatomic potential arising from the polarizabilities of the ions are ignored. Since these contributions are known to play a large role in determining the optical normal-mode frequencies, the question arises of whether or not we can reasonably compare our results with experiment, and, if not, how we are to judge them. This is itself an interesting question since many other calculations of the thermodynamic properties of the alkali halides also used the rigid-ion formalism.[8] If an approximate method of calculation is used even agreement with experiment is not a conclusive test since there may be a cancellation of errors arising from the model and from the method of calculation. In this connection, it is important that the Monte Carlo method is exact within the statistical uncertainties at high temperatures, and that anharmonic perturbation theory converges well for the alkali halides at low temperatures. To anticipate our results, we find that the two methods are in excellent agreement at room temperature, indicating that the two methods together do successfully span the entire temperature range, and also that the agreement with the experimental data is remarkably good. Sodium chloride was chosen as a material to study partly to make connection with earlier calculations, and partly because the measured phonon-dispersion relations[9] indicated that probably only nearest-neighbor non-Coulomb interactions are important.

There have, of course, been earlier Monte Carlo calculations on the alkali halides,[10–12] and we have used the techniques described in that work to deal with the Coulomb potential. However, the computational facilities now available are so superior that we can obtain much more accurate values of the thermodynamic properties than were previously available. It was the usefulness of our earlier benchmark results for the Lennard-Jones solid[2] which suggested the present calculation to us.

II. MODEL POTENTIAL

We assume an interionic potential consisting of Coulomb forces corresponding to the formal ionic charges of $\pm e$, together with a Born-Mayer potential

$$V = V_0 \exp\left[-\frac{r}{\rho}\right], \tag{1}$$

which is assumed to act only between unlike ions. (In the lattice dynamics calculations "unlike" effectively restricted the short-range interaction to nearest neighbors. In the Monte Carlo calculations we found it necessary to include the third-neighbor interactions, since otherwise, at very high temperatures, an ion could be drawn out of its cage of nearest unlike neighbors by the Coulomb attraction of third unlike neighbors leading to an unlimited lowering of the internal energy of the crystal.) The two parameters in the potential were determined from the zero-temperature values of the nearest-neighbor distance r_0 and the bulk modulus B_T. We assumed values of 2.797 24 Å and 2.660×10^{11} dyn/cm^2 for these. As a starting point the derivatives of the static lattice energy were adjusted to correspond to these values, and the parameters were then refined iteratively until the minimum

and the second-volume derivative of the quasiharmonic Helmholtz function yielded the experimental values. Anharmonic corrections to the Helmholtz function are very small at zero degrees. The final values we adopted for V_0 and ρ were $3.221\,774\,3\times10^{-9}$ ergs, and 0.295 01 Å, respectively.

We can find support for this simple model in several places. The measured phonon-dispersion relation,[9] especially the acoustic branches, are well reproduced by a nearest-neighbor model. Also, Boyer[13] has made *a priori* calculations of the interatomic potential in alkali halides, using a density-functional method. He gives the potential as a sum of four contributions, but we have summed them and fitted a single Born-Mayer form to the values in the vicinity of the experimental separations. From the results we can verify that the like-neighbor potentials are very small (e.g., for Cl-Cl, $V_0=-3\times10^{-12}$ ergs and $\rho=1.104\,08$ Å), and we also extract values of V_0 and ρ for unlike nearest neighbors which agree with the values given above to within 6% and 1%, respectively. We view this agreement as excellent.

Many rigid-ion model calculations for the alkali halides, including earlier Monte Carlo[10–12] and molecular-dynamics[14] calculations, have used a set of interatomic potentials derived by Tosi and Fumi.[15] That work was an attempt to derive a universal set of parameters for the alkali halides, with the magnitudes of the repulsive terms determined from a set of ionic radii. van der Waals interactions, between more distant neighbors, were also included. While the Tosi and Fumi potentials do reproduce the low-temperature properties fairly well, the ionic-radius approach to the repulsive terms is inferior to a density-functional approach, and there is no direct evidence for the long-range van der Waals contribution to the potential. Ree and Holt[8] in fact concluded in their work that Tosi and Fumi potentials were inadequate. This same conclusion was also reached by Adams and McDonald.[12] The model we have used is simpler, and actually turns out to agree far better with experiment.

III. ANHARMONIC PERTURBATION THEORY

The well-tried route of anharmonic perturbation theory[16] is to calculate the Helmholtz function as a sum of the static energy, the quasiharmonic (qh) vibrational free energy, and contributions arising in first and second orders of perturbation theory, respectively, containing the quartic and squared cubic terms in the Taylor expansion of the potential energy,

$$F=\Phi_0+F_{\rm qh}+F_4+F_{33}\ . \tag{2}$$

Here

$$F_{\rm qh}=\sum_{\lambda}\left\{\frac{\hbar\omega_\lambda}{2}+kT\ln\left[1-\exp\left[-\frac{\hbar\omega}{kT}\right]\right]\right\}, \tag{3}$$

where the sum is over the $3N$ normal modes of the crystal. At high temperatures F_4 and F_{33} are each proportional to the square of the temperature,

$$F_4=12\frac{k^2T^2}{\hbar^2}\frac{V(\lambda_1,-\lambda_1,\lambda_2,-\lambda_2)}{\omega(\lambda_1)\omega(\lambda_2)}\ , \tag{4}$$

$$F_{33}=-24\frac{k^2T^2}{\hbar^2}\sum_{\lambda_1,\lambda_2,\lambda_3}\frac{|V(\lambda_1,\lambda_2,\lambda_3)|^2}{\omega(\lambda_1)\omega(\lambda_2)\omega(\lambda_3)}\ . \tag{5}$$

The notation is described fully in the review article by Cowley.[16] We had found in our earlier calculations[6,7] that it was a satisfactory compromise to use the finite-temperature expression for the quasiharmonic terms, and only the high-temperature limits for the anharmonic terms, because the anharmonic contributions are small at the temperatures where quantum-mechanical corrections would be important. Our numerical techniques were similar to the previous work, in particular the sums in F_{33} were carried out over a mesh of 256 wave vectors. The one improvement was that the Coulumb contributions to $V(\lambda_1,\lambda_2,\lambda_3)$ were summed using an Ewald procedure which gave an essentially exact result.

In order to find the zero-pressure volume, and the various thermodynamic properties, as functions of temperature, the two anharmonic coefficients of T^2 were each calculated at eleven volumes, and cubic spline interpolation was used. The quasiharmonic contributions to the free energy, entropy, and heat capacity C_v were calculated at each volume as required.

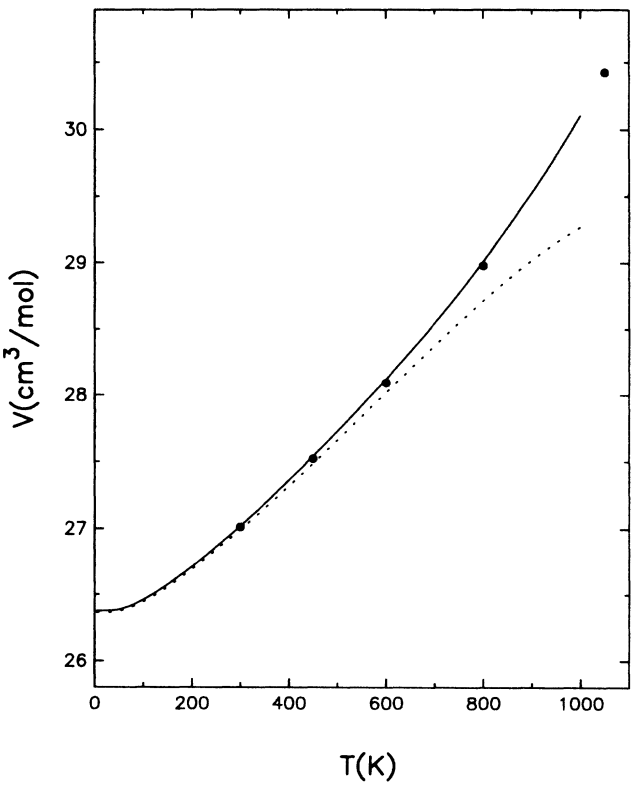

FIG. 1. Molar volume of NaCl as a function of temperature at zero pressure. Solid circles, Monte Carlo simulations with 4.172×10^6 configurations, except at 1050 K where we used 1.0368×10^7 configurations; dotted line, anharmonic lattice dynamics; solid line, smoothed experimental data (Ref. 20).

IV. MONTE CARLO SIMULATIONS

The basic Monte Carlo method has been described by Wood,[17] and its application to the alkali halides has been discussed by Woodcock and co-workers[10,11] and by Adams and McDonald.[12] The main difference between our procedure and theirs is that we used an N-V-T ensemble, and adjusted the volume iteratively until the pressure was calculated to be zero within the statistical uncertainty. This is a brute-force solution to the difficulty mentioned by Adams and McDonald, that the short-range part of the energy cannot be exactly scaled if the sample volume is altered in an N-P-T ensemble. We also included the first term of the Wigner-Kirkwood correction for quantum-mechanical effects.[18] Our production runs were carried out for a system of 216 ions, and with the real-space part of the Ewald summation for the Coulomb energy including all neighbors within a distance of $r_c = L/2$. The parameter α,[10,11] which divides the Ewald sum between real space and reciprocal space, was chosen[12] so that $\alpha L = 5.05$, and the reciprocal space sum was taken over 128 reciprocal lattice vectors for which $0 < |\mathbf{n}|^2 \leq l_c = 16$. Of course, we also used periodic boundary condition.

As some compensation for the small sample size, we used a correction described in Ref. 2. This involves calculating separately the static and vibrational contributions to the various averages and assuming that the vibrational parts are proportional to $N-1$ instead of N. In the application to the Coulomb sums this has the added advantage that the static terms can be calculated once and for all to a very high degree of convergence, so that overall accuracy is improved. To test the adequacy of this correction, we also performed runs with a system of 64 atoms, and verified that the changes in the normalized averages were comparable with the statistical uncertainties.

Also, with a 64-atom sample, it was possible to repeat some runs with a much larger α parameter in the Ewald sums to maintain the same value for αL as for the 216-ion sample. The reciprocal-space sum must then be extended over a larger radius so that this is an expensive procedure, but we were able to verify that the increased accuracy in the Ewald sums changed the calculated thermodynamic quantities only by amounts comparable with the statistical uncertainties.

The production runs were carried out at five temperatures, ranging from 300 to 1050 K. Each run was continued for 4.172×10^6 configurations, of which the first 4.32×10^4 were discarded. The statistical uncertainties were calculated by breaking the chain of configurations into a number of smaller blocks (typically about 10),

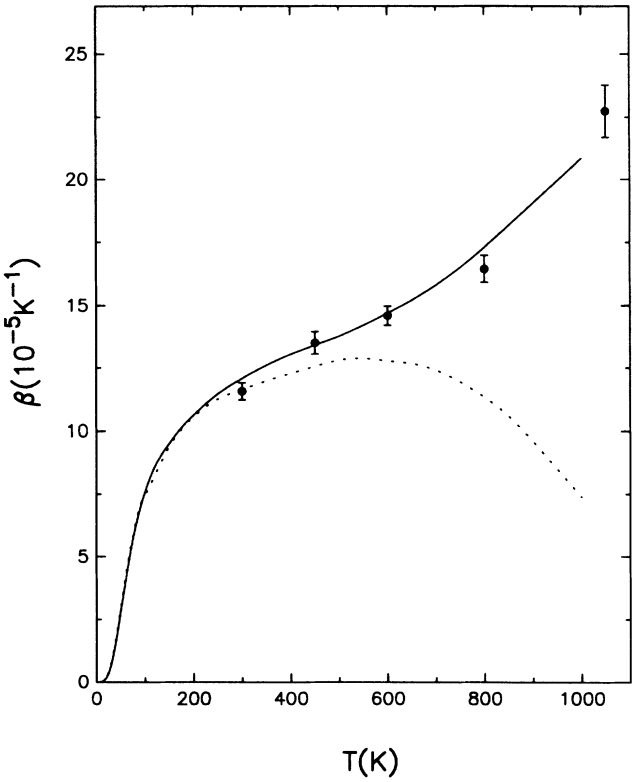

FIG. 2. Zero-pressure volume expansivity of NaCl as a function of temperature. Solid circles, Monte Carlo simulations with 4.172×10^6 configurations, except at 1050 K where we used 1.0368×10^7 configurations; dotted line, anharmonic lattice dynamics; solid line, smoothed experimental data (Ref. 20).

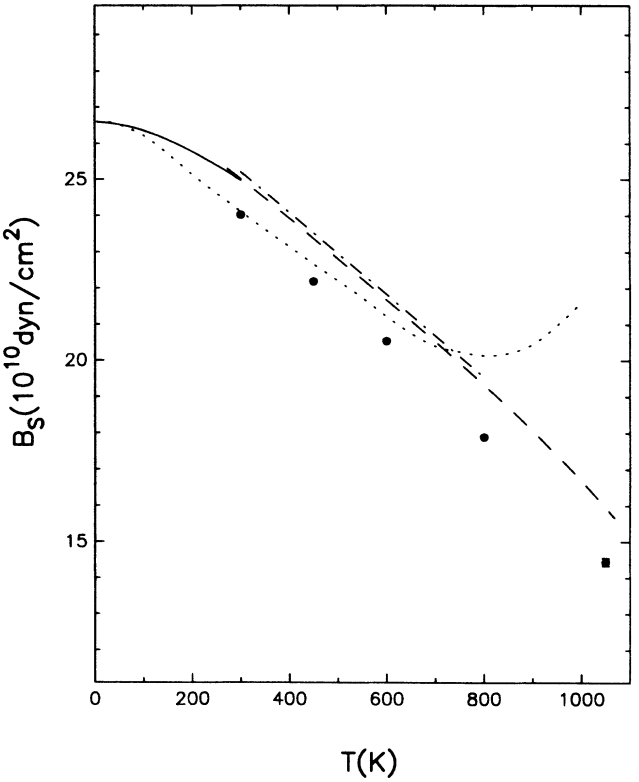

FIG. 3. Zero-pressure adiabatic bulk modulus of NaCl as a function of temperature. Solid circles, Monte Carlo simulations with 4.172×10^6 configurations, except at 1050 K where we used 1.0368×10^7 configurations; dotted line, anharmonic lattice dynamics; solid line, smoothed experimental data (Ref. 21); dashed line, smoothed experimental data (Ref. 22); dotted-dashed line, smoothed experimental data (Ref. 26).

which were treated as independent. The uncertainties obtained in this way were completely in accordance with the uncertainties obtained in Ref. 2, when allowance is made for the different sample size and number of configurations. They were also consistent with the variations observed when several runs were performed at the same temperature but at slightly different volumes, during the iterations to find the zero-pressure volume.

An interesting difficulty we encountered has been mentioned earlier. The repulsive part of our model potential acts only between unlike ions, and in our Monte Carlo calculation we initially included it only between nearest neighbors. This was satisfactory at 300 and 450 K, but at the higher temperatures the crystal became unstable, sometimes only after more than a million configurations had been generated. The resolution of the difficulty was to include the repulsive interaction between third unlike neighbors, since it was the uncompensated Coulomb attraction between these neighbors which was causing the instability. The contribution of these third-neighbor forces between unlike neighbors in the lattice dynamical calculation were found to be quite small, much less than 1%. In the Monte Carlo simulation, however, at high T, some large ionic displacements were inevitable. Therefore close encounters with unlike third neighbors must be allowed for so that they do not overpower all the many less drastic moves.

Because of the long-range Coulomb forces in ionic solids, conventional expressions for the elastic constants must be adapted for use in Monte Carlo calculations. We start with the general expression

$$Vc^{T}_{\alpha\beta\gamma\delta} = \left[\frac{\partial^2 F}{\partial \eta_{\alpha\beta} \partial \eta_{\gamma\delta}} \right]_T , \tag{6}$$

with

$$F = -3NkT \ln \left[\left[\frac{kT}{2\pi\hbar^2} \right]^{1/2} (m_{\mathrm{Na}} m_{\mathrm{Cl}})^{1/4} V^{1/3} \right] + 2kT \ln \left[\left[\frac{N}{2} \right] ! \right] - kT \ln \left[\int \cdots \int \exp \left[-\frac{U}{kT} \right] d\tau_1 \cdots d\tau_N \right] + \hbar^2 \langle U_Q \rangle \tag{7}$$

and

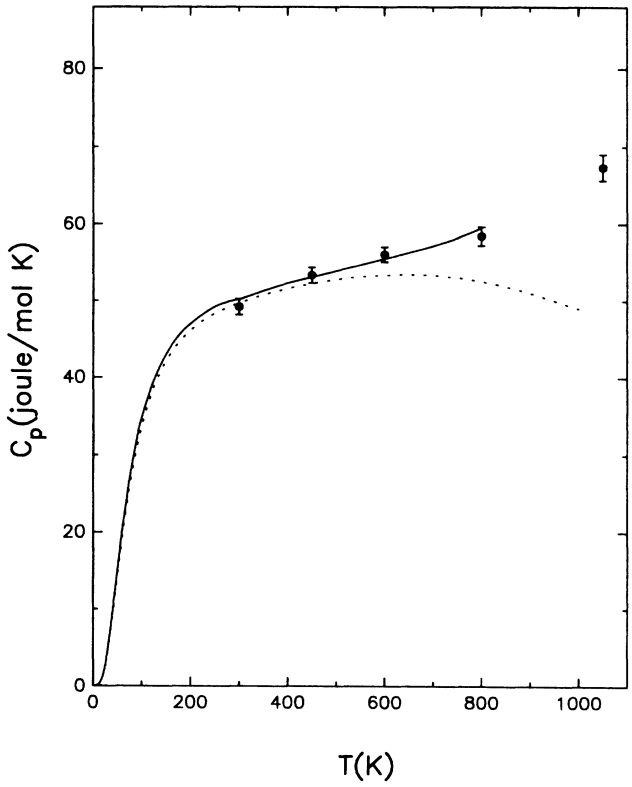

FIG. 4. Zero-pressure molar specific heat of NaCl, at constant pressure, as a function of temperature. Solid circles, Monte Carlo simulations with 4.172×10^6 configurations, except at 1050 K where we used 1.0368×10^7 configurations; dotted line, anharmonic lattice dynamics; solid line, smoothed experimental data (Refs. 23 and 24).

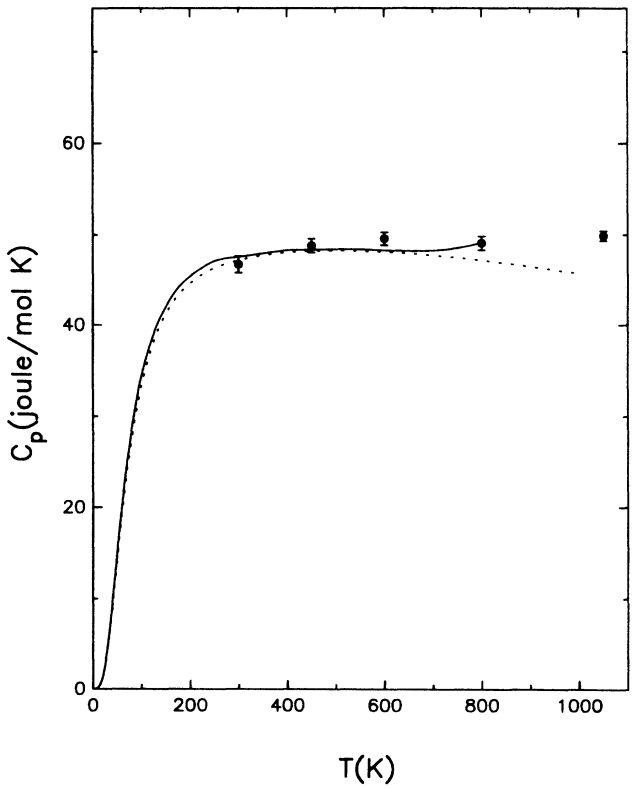

FIG. 5. Zero-pressure molar specific heat of NaCl at constant volume as a function of temperature. Solid circles, Monte Carlo simulations with 4.172×10^6 configurations, except at 1050 K where we used 1.0368×10^7 configurations; dotted line, anharmonic lattice dynamics; solid line, from smoothed experimental data (Refs. 21–24).

$$U_Q=\frac{1}{24kT}\sum_i\frac{\nabla_i^2 U}{m_i}=\frac{1}{24kT}\sum_i\frac{\nabla_i^2 U(S)}{m_i}\ ,$$

$$VC_{\alpha\beta}^T=\left[\frac{\partial F}{\partial\eta_{\alpha\beta}}\right]_T$$
$$=-NkT\frac{\partial\ln V}{\partial\eta_{\alpha\beta}}+\left\langle\frac{\partial U}{\partial\eta_{\alpha\beta}}\right\rangle+\hbar^2\left\langle\frac{\partial U_Q}{\partial\eta_{\alpha\beta}}\right\rangle$$
$$+\frac{\hbar^2}{kT}\left[\langle U_Q\rangle\left\langle\frac{\partial U}{\partial\eta_{\alpha\beta}}\right\rangle-\left\langle U_Q\frac{\partial U}{\partial\eta_{\alpha\beta}}\right\rangle\right]\ , \quad (8)$$

where $\langle\ \rangle$ denotes the ensemble average. There are three distinct contributions to U—the short-range part $U(S)$, the real-space Coulomb sum $U(C_1)$, and the reciprocal space Coulomb sum $U(C_2)$:

$$U(S)=\sum_{i<j}V_0\exp\left[-\frac{r_{ij}}{\rho}\right]\ , \quad (9)$$

$$U(C_1)=\sum_i Z_i\sum_{j>i}Z_j\frac{\mathrm{erfc}(\alpha r_{ij})}{r_{ij}}-\sum_i\frac{\alpha Z_i^2}{\sqrt{\pi}}\ , \quad (10)$$

$$U(C_2)=\tfrac{1}{2}\sum_{\mathbf{n}}{}'C(\mathbf{n})\ ,$$

where

$$Z_i=\pm e\ ,$$

and

$$C(\mathbf{n})=\frac{1}{\pi|\mathbf{n}|^2L}\exp\left[-\frac{\pi^2|\mathbf{n}|^2}{\alpha^2L^2}\right]$$
$$\times\left\{\left[\sum_i Z_i\cos\left[2\pi\frac{\mathbf{n}\cdot\mathbf{r}_i}{L}\right]\right]^2\right.$$
$$\left.+\left[\sum_i Z_i\sin\left[2\pi\frac{\mathbf{n}\cdot\mathbf{r}_i}{L}\right]\right]^2\right\}\ . \quad (11)$$

It is straightforward to include the contributions of Eqs. (9) and (10) to Eq. (8), using the formula of Ref. 19. Those of Eq. (11) are

$$\frac{\partial U(C_2)}{\partial\eta_{\alpha\beta}}=-\delta_{\alpha\beta}U(C_2)$$
$$+\sum_{\mathbf{n}}{}'n_\alpha n_\beta\left[\frac{1}{|\mathbf{n}|^2}+\frac{\pi^2}{\alpha^2L^2}\right]C(\mathbf{n})\ . \quad (12)$$

Finally, using Eq. (6) we find that

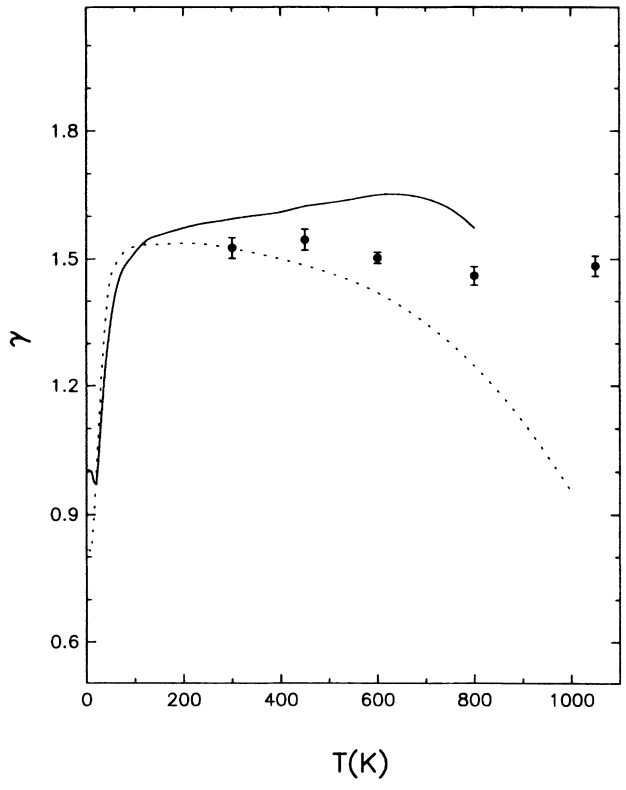

FIG. 6. Grüneisen's parameter γ for NaCl, at zero pressure, as a function of temperature. Solid circles, Monte Carlo simulations with 4.172×10^6 configurations, except at 1050 K where we used 1.0368×10^7 configurations; dotted line, anharmonic lattice dynamics; solid line, smoothed experimental data (Refs. 20–24).

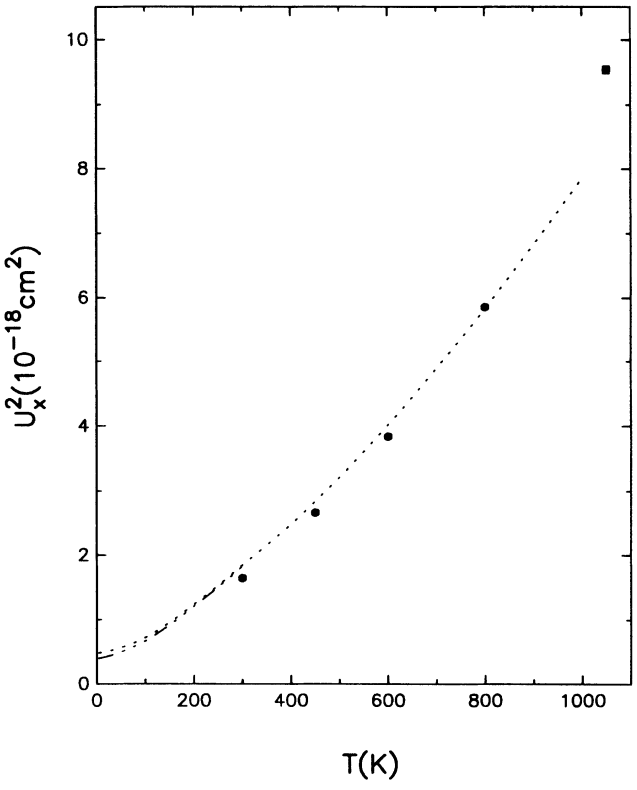

FIG. 7. Zero-pressure mean square deviation of an ion in NaCl as a function of temperature. Solid circles, Monte Carlo simulations with 4.172×10^6 configurations, except at 1050 K where we used 1.0368×10^7 configurations; dotted line, anharmonic lattice dynamics. Below 300 K, the dashed–triple-dotted line shows the mean square deviation of a chlorine ion, and the dotted line shows that of a sodium ion.

$$
\begin{aligned}
Vc^{T}_{\alpha\beta\gamma\delta} = & \frac{1}{kT}\left[\left\langle\frac{\partial U}{\partial\eta_{\alpha\beta}}\right\rangle\left\langle\frac{\partial U}{\partial\eta_{\gamma\delta}}\right\rangle-\left\langle\frac{\partial U}{\partial\eta_{\alpha\beta}}\,\frac{\partial U}{\partial\eta_{\gamma\delta}}\right\rangle\right]+\left\langle\frac{\partial^2 U_Q}{\partial\eta_{\alpha\beta}\partial\eta_{\gamma\delta}}\right\rangle+2NkT\delta_{\alpha\beta}\delta_{\beta\gamma}+\hbar^2\left\langle\frac{\partial^2 U_Q}{\partial\eta_{\alpha\beta}\partial\eta_{\gamma\delta}}\right\rangle \\
& +\frac{\hbar^2}{kT}\left[\left\langle\frac{\partial U}{\partial\eta_{\alpha\beta}}\right\rangle\left\langle\frac{\partial U_Q}{\partial\eta_{\gamma\delta}}\right\rangle+\left\langle\frac{\partial U}{\partial\eta_{\gamma\delta}}\right\rangle\left\langle\frac{\partial U_Q}{\partial\eta_{\alpha\beta}}\right\rangle-\left\langle\frac{\partial U}{\partial\eta_{\alpha\beta}}\,\frac{\partial U_Q}{\partial\eta_{\gamma\delta}}\right\rangle-\left\langle\frac{\partial U_Q}{\partial\eta_{\alpha\beta}}\,\frac{\partial U}{\partial\eta_{\gamma\delta}}\right\rangle\right. \\
& \left.+\langle U_Q\rangle\left\langle\frac{\partial^2 U}{\partial\eta_{\alpha\beta}\partial\eta_{\gamma\delta}}\right\rangle-\left\langle U_Q\,\frac{\partial^2 U}{\partial\eta_{\alpha\beta}\partial\eta_{\gamma\delta}}\right\rangle\right] \\
& +\frac{\hbar^2}{k^2T^2}\left[2\langle U_Q\rangle\left\langle\frac{\partial U}{\partial\eta_{\alpha\beta}}\right\rangle\left\langle\frac{\partial U}{\partial\eta_{\gamma\delta}}\right\rangle-\left\langle U_Q\,\frac{\partial U}{\partial\eta_{\alpha\beta}}\right\rangle\left\langle\frac{\partial U}{\partial\eta_{\gamma\delta}}\right\rangle-\langle U_Q\rangle\left\langle\frac{\partial U}{\partial\eta_{\alpha\beta}}\,\frac{\partial U}{\partial\eta_{\gamma\delta}}\right\rangle\right. \\
& \left.+\left\langle U_Q\,\frac{\partial U}{\partial\eta_{\alpha\beta}}\,\frac{\partial U}{\partial\eta_{\gamma\delta}}\right\rangle-\left\langle\frac{\partial U}{\partial\eta_{\alpha\beta}}\right\rangle\left\langle U_Q\,\frac{\partial U}{\partial\eta_{\gamma\delta}}\right\rangle\right] . \qquad (13)
\end{aligned}
$$

Again, the contributions of Eqs. (9) and (10) to Eq. (13) are straightforward. Those of Eq. (11) are

$$
\begin{aligned}
\frac{\partial^2 U(C_2)}{\partial\eta_{\alpha\beta}\partial\eta_{\gamma\delta}} = & (2\delta_{\alpha\delta}\delta_{\beta\gamma}+\delta_{\alpha\beta}\delta_{\gamma\delta})U(C_2)+\sum_{\mathbf{n}}{}'\left\{4n_\alpha n_\beta n_\gamma n_\delta\left[\frac{1}{|\mathbf{n}|^2}\left[\frac{1}{|\mathbf{n}|^2}+\frac{\pi^2}{\alpha^2L^2}\right]+\frac{\pi^4}{2\alpha^4L^4}\right]\right. \\
& -[n_\alpha n_\beta\delta_{\gamma\delta}+n_\gamma n_\delta\delta_{\alpha\beta}+2(\delta_{\alpha\delta}n_\beta n_\gamma+\delta_{\beta\gamma}n_\alpha n_\delta)] \\
& \left.\times\left[\frac{1}{|\mathbf{n}|^2}+\frac{\pi^2}{\alpha^2L^2}\right]\right\}C(\mathbf{n}) . \qquad (14)
\end{aligned}
$$

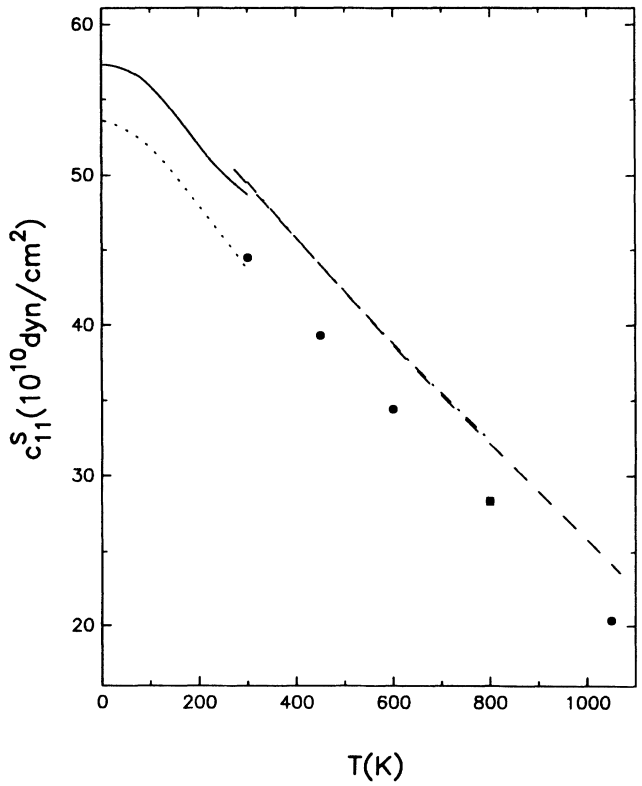

FIG. 8. Adiabatic elastic constant c_{11}^S as a function of temperature. Solid circles, Monte Carlo simulations with 4.172×10^6 configurations, except at 1050 K where we used 1.0368×10^7 configurations; dotted line, lattice dynamics; solid line, smoothed experimental data (Ref. 21); dashed line, smoothed experimental data (Ref. 22); dotted-dashed line, smoothed experimental data (Ref. 26).

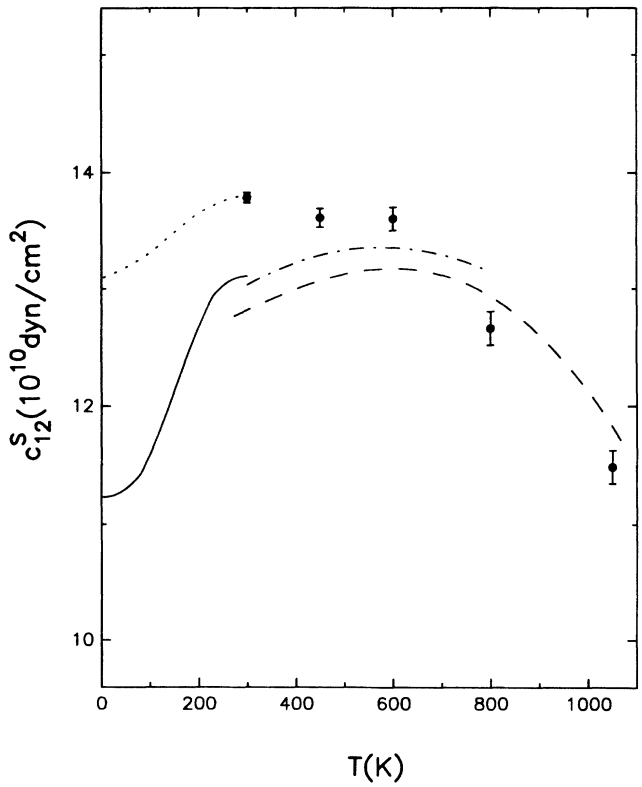

FIG. 9. Adiabatic elastic constant c_{12}^S as a function of temperature. Solid circles, from Monte Carlo simulations with 4.172×10^6 configurations, except at 1050 K where we used 1.0368×10^7 configurations; dotted line, lattice dynamics; solid line, smoothed experimental data (Ref. 21); dashed line, smoothed experimental data (Ref. 22); dotted-dashed line, smoothed experimental data (Ref. 26).

V. RESULTS AND DISCUSSIONS

Figures 1–6 show our results for the cell-volume, volume thermal expansivity β, adiabatic bulk modulus B_S, specific heat at constant pressure C_p, specific heat at constant volume C_v, and the Grüneisen parameter γ. In each case, the dashed lines show the lattice dynamics results, the solid circles with error bars are the Monte Carlo results, and the solid line has been drawn through the experimental values. The experimental data are from Refs. 20–25.

The error bars on the Monte Carlo results are purely statistical uncertainties, but we believe these to be the major contribution, compared with errors due to small sample size and termination of the Ewald sums. The errors in the other sets of results are more likely to be systematic, leading to an upward or downward shift of the entire curve. The sums over the Brillouin zone involved in the lattice-dynamics values were all carried out to accuracies much better than the size of the plotted points. The interpolations and numerical differentiations required to form the equation of state reduce this accuracy, but we believe that even our results for β and C_v at 300 K, for example, are accurate to 1% and 0.2%, respectively. The experimental curves each have their own uncer-

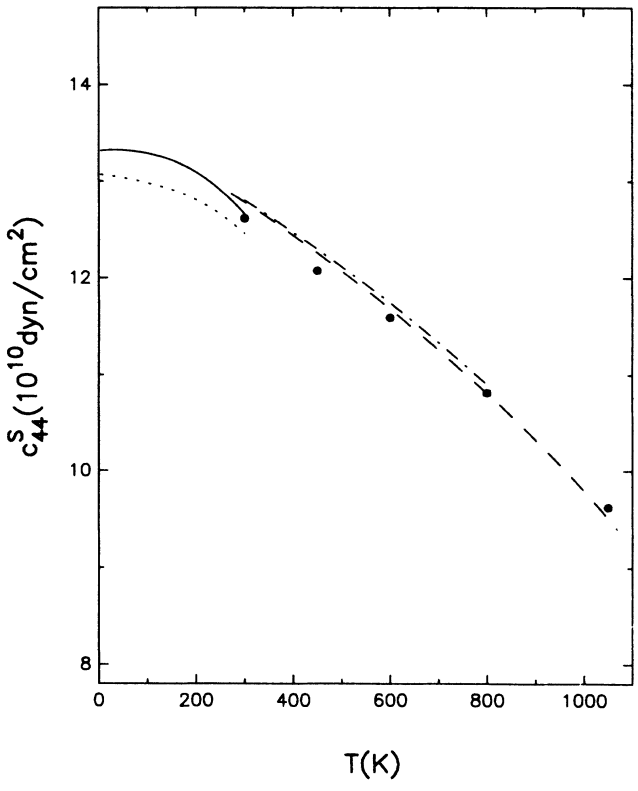

FIG. 10. Adiabatic elastic constant c_{44} as a function of temperature. Solid circles, Monte Carlo simulations with 4.172×10^6 configurations, except at 1050 K where we used 1.0368×10^7 configurations; dotted line, lattice dynamics; solid line from smoothed experimental data (Ref. 21); dashed line, smoothed experimental data (Ref. 22); dotted-dashed line, smoothed experimental data (Ref. 26).

TABLE I. Temperature dependence of zero-pressure thermodynamic functions for NaCl. The uncertainty represents the standard error of the mean. All the Monte Carlo results correspond to 4.172×10^6 configurations except the numbers in parentheses, which correspond to 1.0368×10^7 configurations.

	T (K)	V (cm^3/mol)	P (bars)	E (10^3 J/mol)	C_v (J/mol K)	C_p (J/mol K)	γ	β (10^{-5} K^{-1})	u_x^2 (10^{-18} cm^2) Na	Cl
Lattice dynamics	0	26.361	0	−773.56	0	0	0.828	0	0.480	0.394
	100	26.444	0	−772.08	33.38	33.76	1.529	7.44	0.723	0.670
	200	26.692	0	−767.94	44.63	46.07	1.537	10.55	1.241	1.211
	300	26.991	0	−763.12	47.21	49.72	1.524	11.65	1.845	1.825
Monte Carlo	300	27.013	−4±13	−763.07±0.01	46.7±0.9	49.2±1.0	1.53±0.02	11.6±0.3	1.646±0.007	1.644±0.006
	450	27.522	−13±20	−755.39±0.02	48.8±0.8	53.4±1.0	1.55±0.03	13.5±0.4	2.66±0.01	2.659±0.009
	600	28.094	−10±29	−747.27±0.03	49.6±0.7	56.0±1.0	1.50±0.01	14.6±0.4	3.84±0.02	3.85±0.02
	800	28.980	9±58	−735.87±0.05	49.1±0.8	58.4±1.2	1.46±0.02	16.5±0.5	5.86±0.03	5.84±0.03
	1050	30.424	−62±83	−720.12±0.10	50.1±0.9	68.9±2.7	1.52±0.02	23.8±1.6	9.54±0.09	9.55±0.12
	1050	30.424	(−54±43)	(−720.12±0.04)	(49.9±0.5)	(67.3±1.7)	(1.48±0.02)	(22.7±1.0)	(9.53±0.05)	(9.54±0.06)

tainties. The absolute accuracy of the volume thermal expansivity is stated to be 7%, and that of C_p is 0.3–0.5%. The bulk modulus is accurate to about 2% and the accuracy of the Grüneisen parameter is about 7%.

Bearing in mind these uncertainties, it is not too strong a statement to say that the lattice-dynamics calculations up to 300 K and the Monte Carlo calculation from 300 K to melting are in agreement with the experimental results for all of the properties. Considering the simple model potential used, we find this result remarkable. As expected, for high temperatures the lattice-dynamics results diverge from those of the Monte Carlo simulations. For critical comparison the deviation begins at 300 K, but the results are still fairly reasonable up to about half the melting temperature. It is worth noting in Fig. 2 that both theory and experiment are consistent with the Dulong and Petit value ($C_v = 6R$) at high T.

We have also calculated the mean-square displacements of the two ions. They are almost identical at high T. In our Monte Carlo procedure the center of mass of the systems drifts free, and the equilibrium positions of the ions move with it. We therefore maintained a running value of the positions of the center of mass, and found the averages of the squared displacements of the ions from their drifting equilibrium positions. The same procedure proved satisfactory in an earlier calculation.[26] The results are shown in Fig. 7. We also show there values calculated using the quasiharmonic lattice-dynamical expressions, but calculated at the equilibrium volumes predicted by the full lattice-dynamical theory. Both curves are approximations. The Monte Carlo results are more sensitive to the small sample size than were the thermodynamic results, and the lattice-dynamics results do not include anharmonic corrections. However, this is a notoriously difficult quantity to measure, and we believe that these results can be quite useful.

The adiabatic elastic constants obtained in the Monte Carlo calculations are shown in Figs. 8–10, compared with the experimental results of Refs. 21, 22, and 25. A useful discussion of elastic constants of NaCl can be found in the paper by Benkert and Backstrom.[27] Also shown there are values calculated by the method of Ree and Holt,[8] as second derivatives of the quasiharmonic free energy with respect to strains. Above 300 K, this method becomes unreliable because of the anharmonic terms omitted from the free energy. The immediate problem is that the volumes corresponding to zero pressure rapidly becomes unreasonable above room temperature when only the quasiharmonic free energy is used.[28] The Monte Carlo and lattice-dynamical results for the elastic constants agree nicely in the overlap region, as expected. Our results differ widely from those of Ree and Holt[8] and this is due to the potential used by them. Our results agree far better with experiment. Our results for c_{12} and c_{44} agree with the experiments, except for c_{12} below room temperature. The drop in c_{12} at the lowest temperatures is clearly due to three-body forces. These are included in our model in an effective way via the fitted parameters of our Born-Mayer two-body potential. Since our model fitted the bulk modulus at zero degrees, our model forces the low-temperature discrepancy in c_{12}. The inclusion of three-body forces,[29] rather than using a shell model, to account for this low-temperature discrepancy remains to be investigated. The effect is clearly temperature dependent and, as is clear from Fig. 9, has disappeared at about half the melting temperature when the crystal has expanded sufficiently for the overlap effect involved to fade out.

As is well known, there are deviations from the Cauchy relation, $c_{12} = c_{44}$, in the alkali halides at low temperatures, and this indicates the presence of three-body forces. Since our model does not include these forces it leads to $c_{12} \sim c_{44}$. However, at finite temperatures a part of the deviations from the Cauchy relation is caused by anharmonicity, and the experimental results show that the deviation from the Cauchy relation changes sign a little below room temperature. Since anharmonic effects are negligible at low T, we conclude that the contribution of three-body forces to c_{12}-c_{44} is of the opposite sign to that of the anharmonic contribution, and the latter, as expected, is the larger at high T.

Finally, in view of the benchmark nature to which we hope our results will be put, we give in Tables I–III a summary of our Monte Carlo and lattice-dynamics results for the thermodynamic and elastic properties. In a future paper we shall use these to test cell and cell-cluster calculations for the model.

TABLE II. Zero-pressure elastic functions for NaCl as a function of temperature. The uncertainty represents the standard error of the mean. All the Monte Carlo results correspond to 4.172×10^6 configurations except the numbers in parentheses which correspond to 1.0368×10^7 configurations.

	T (K)	B_T	B_S	c_{11}^T	c_{11}^S (10^{10} dyn/cm^2)	c_{12}^T	c_{12}^S	c_{44}
Lattice dynamics	0	26.60	26.60	53.60	53.60	13.09	13.09	13.07
	100	25.93	26.22	51.52	51.84	13.00	13.31	12.98
	200	24.35	25.13	47.70	47.95	12.76	13.65	12.81
	300	22.88	24.10	42.25	43.70	12.35	13.81	12.46
Monte Carlo	300	22.82±0.06	24.02±0.03	43.30±0.06	44.50±0.04	12.58±0.07	13.78±0.04	12.615±0.008
	450	20.3±0.1	22.18±0.05	37.4±0.2	39.3±0.1	11.7±0.1	13.61±0.08	12.075±0.009
	600	18.2±0.1	20.54±0.08	32.0±0.1	34.4±0.1	11.2±0.1	13.6±0.1	11.58±0.01
	800	15.0±0.1	17.89±0.05	25.5±0.2	28.3±0.2	9.8±0.2	12.7±0.1	10.81±0.03
	1050	10.5±0.4	14.4±0.2	16.5±0.3	20.5±0.2	7.5±0.4	11.4±0.3	9.62±0.03
	1050	(10.7±0.2)	(14.4±0.1)	(16.6±0.3)	(20.4±0.2)	(7.7±0.2)	(11.5±0.1)	(9.63±0.02)

TABLE III. Dependence of certain thermodynamic and elastic functions for NaCl on crystal size and treatment of the Coulomb forces. $T=800$ K, $\alpha L=5.05$. The uncertainty represents the standard error of the mean. $L=6a$ corresponds to 216 atoms and $L=4a$ corresponds to 64 atoms.

Property	$L=6a$, $a=2.8870$ Å $r_c=L/2$, $l_c=16$	$L=4a$, $a=2.8859$ Å $r_c=L/2$, $l_c=16$	$L=4a$, $a=2.8859$ Å $r_c=3L/4$, $l_c=49$
E (10^3 J/mol)	-735.87 ± 0.05	-736.03 ± 0.08	-735.96 ± 0.08
P (bars)	9 ± 58	-31 ± 61	7 ± 98
C_v (J/mol K)	49.1 ± 0.8	48.2 ± 1.1	49.6 ± 0.5
C_p (J/mol K)	58.4 ± 1.2	57.3 ± 2.0	60.0 ± 0.7
γ	1.46 ± 0.02	1.46 ± 0.03	1.51 ± 0.02
β (10^{-5} K^{-1})	16.5 ± 0.5	16.2 ± 0.9	17.7 ± 0.4
u_x^2 (10^{-18} cm^2)			
Na	5.86 ± 0.03	5.13 ± 0.04	5.15 ± 0.03
Cl	5.84 ± 0.03	5.09 ± 0.03	5.11 ± 0.04
B_T (10^{10} dyn/cm^2)	15.0 ± 0.1	15.0 ± 0.2	14.6 ± 0.1
B_S	17.89 ± 0.05	17.8 ± 0.1	17.70 ± 0.06
c_{11}^T	25.5 ± 0.2	24.9 ± 0.3	24.9 ± 0.2
c_{11}^S	28.3 ± 0.2	27.7 ± 0.3	27.9 ± 0.2
c_{12}^T	9.8 ± 0.2	10.1 ± 0.2	9.5 ± 0.1
c_{12}^S	12.7 ± 0.1	12.9 ± 0.1	12.6 ± 0.1
c_{44}	10.81 ± 0.03	10.89 ± 0.03	10.92 ± 0.02

We note that our lowest-order anharmonic perturbation theory lattice-dynamical results are satisfactory to higher temperatures, half the melting temperature, than is usual in other classes of solids.[30] This is due to the fortuitous near cancellation between F_4 and F_{33}. Our benchmark results can now be used to ascertain if a lattice-dynamical theory can be devised, either by including higher-order anharmonic effects perturbatively or self-consistently, that holds up to the melting point. Indeed, it may be necessary to include short-range correlations[4] in a self-consistent lattice dynamics to give agreement with the Monte Carlo results presented in Table I–III.

ACKNOWLEDGMENTS

We would like to thank the John von Neumann National Supercomputer Center for access to the CYBER 205 under Grant No. LAC 23080.

[1]R. C. Shukla and E. R. Cowley, Phys. Rev. B **31**, 372 (1985).
[2]E. R. Cowley, Phys. Rev. B **28**, 3160 (1983).
[3]M. L. Klein, J. A. Barker, and T. R. Koehler, Phys. Rev. B **4**, 1983 (1971).
[4]E. R. Cowley and G. K. Horton, Phys. Rev. Lett. **58**, 789 (1987).
[5]M. L. Klein and R. D. Murphy, Phys. Rev. B **6**, 2433 (1972).
[6]E. R. Cowley, J. Phys. C. **4**, 988 (1971).
[7]E. R. Cowley, J. Phys. C **5**, 1345 (1972).
[8]L. L. Boyer, Phys. Rev. Lett. **42**, 584 (1979). See also F. H. Ree and A. C. Holt, Phys. Rev. B **8**, 826 (1973). For a general review see the articles by J. R. Hardy and by H. Bilz *et al.*, in *Dynamical Properties of Solids*, edited by G. K. Horton and A. A. Maradudin (North-Holland, Amsterdam, 1974).
[9]G. Raunio, L. Alnqvist, and R. Stedman, Phys. Rev. **178**, 1496 (1969).
[10]L. V. Woodcock and K. Singer, Trans. Faraday Soc. **67**, 12 (1971).
[11]J. W. E. Lewis, K. Singer, and L. V. Woodcock, J. Chem. Soc. Faraday II **71**, 301 (1975).
[12]D. J. Adams and I. R. McDonald, J. Phys. C **7**, 276 (1974).
[13]L. L. Boyer, Phys. Rev. Lett. **45**, 1858 (1980).
[14]E. R. Cowley, G. Jacucci, M. L. Klein, and I. R. McDonald, Phys. Rev. B **14**, 1758 (1976).
[15]M. P. Tosi and F. G. Fumi, J. Phys. Chem. Solids **25**, 45 (1964).
[16]R. A. Cowley, Adv. Phys. **12**, 421 (1963).
[17]W. W. Wood, in *Physics of Simple Liquids*, edited by H. N. V. Temperley, J. S. Rowlinson, and G. S. Rushbrooke (North-Holland, Amsterdam, 1968).
[18]E. Wigner, Phys. Rev. **40**, 749 (1932).
[19]D. R. Squire, A. C. Holt, and W. G. Hoover, Physica (Utrecht) **42**, 388 (1969).
[20]*Thermal Expansion of Non-Metallic Solids*, Vol. 13 of *Thermophysical Properties of Matter*, edited by Y. S. Touloukian and C. Y. Ho (Plenum, New York, 1977).
[21]J. T. Lewis, A. Lehoozky, and C. V. Briscoe, Phys. Rev. **161**, 877 (1967).
[22]O. D. Slagle and H. A. McKinstry, J. Appl. Phys. **38**, 437 (1967).
[23]T. H. K. Barron, A. J. Leadbetter, and J. A. Morrison, Proc. R. Soc. London, Ser. A **279**, 62 (1964).
[24]A. J. Leadbetter and G. R. Settatree, J. Phys. C **2**, 385 (1969).
[25]H. Spetzler, C. G. Sammis and R. J. O'Connell, J. Phys.

Chem. Solids **33**, 1727 (1972).
[26]G. A. Heiser, R. C. Shukla, and E. R. Cowley, Phys. Rev. B **33**, 2158 (1986).
[27]L. Benkert and Backstrom, Phys. Scr. **11**, 43 (1975).
[28]M. L. Klein, G. K. Horton and V. V. Goldman, Phys. Rev. B **2**, 4995 (1970).
[29]R. K. Singh and N. P. Verma, Phys. Rev. B **2**, 4288 (1970).
[30]M. L. Klein and G. K. Horton, in *Proceedings of the International Conference on Low Temperature Physics–LT-11, St. Andrews, 1968,* edited by J. F. Allen, D. M. Finlayson, and D. M. McCall (St. Andrews University Press, St. Andrews, Scotland, 1968), Vol. 1, p. 553.